Measuring the Site-Specific Reactivity of Impurities: The Pronounced Effect of Dissolved Oxygen on Silicon Etching†

Simon P. Garcia, Hailing Bao, Muthiah Manimaran, and Melissa A. Hines*

Department of Chemistry, Cornell University, Ithaca, New York 14853-1301

Received: March 13, 2002; In Final Form: June 6, 2002

The reactivity of dissolved O_2, a ubiquitous impurity in aqueous solutions, with H-terminated Si(111) surfaces was quantified using a new technique that exploits kinetic competition between an impurity and an etchant to produce impurity-concentration-dependent changes in the steady-state etch morphology. This method is applicable to any impurity that alters the etch morphology. The impurity-induced changes are quantified using scanning tunneling microscopy measurements and atomistic, concentration-dependent kinetic Monte Carlo simulations. The site-specific reactivity of O_2(aq) is surprisingly anisotropic. Oxidation of the highly strained dihydride step site is 4 times faster than oxidation of the relatively unstrained monohydride step site. Both steps are 10^4 times more reactive than terrace sites. The observed site-specific reaction rates are highly correlated to local strain. FTIR measurements of the Si−H stretch vibration showed that dissolved O_2 inserts O atoms into surface Si−Si back-bonds without removing the H-termination. Dissolved O_2 does not attack Si−H bonds, because neither Si−H consumption nor silanol production is observed.

I. Introduction

Defect and impurity reactions are the bane of surface chemists. Although impressive strides have been made in the development of surface spectroscopies, the detection of transient surface species or species present in densities less than a few percent of a monolayer remains challenging. Nevertheless, many reactions occur primarily at defects sites. Growth and etching reactions, in particular, have long been known to be defect-dominated. For example, a typical "flat" Si(111) surface might have a miscut of 0.3°, which corresponds to a vicinal step spacing of ∼500 Å. If an etchant preferentially attacks step sites, only 0.6% of an as-cut surface will be reactive! Impurities present a similar challenge. Although impurities are known to profoundly affect many growth[1] and etching[2] processes, little is known about the site-specific reactivity of impurities or about the chemical mechanism that drives impurity reactions.

In this work, we use a new technique for the quantification of impurity reactivity that combines the high defect sensitivity of scanning tunneling microscopy (STM) with the analytic capabilities of atomistic kinetic Monte Carlo simulations. The site-specific reactivity of an impurity is quantified by kinetic competition with a reference etchant of known reactivity. In the absence of the impurity, the steady-state etch morphology is determined by the site-specific reactivity of the pure etchant. When the impurity is introduced, two reaction channels are active: an etchant channel and an impurity-induced channel. The relative importance of these two channels is controlled by the impurity concentration. Because of this, the site-specific rates of impurity attack can be extracted from an impurity-concentration-dependent study of the steady-state etch morphology.

Hydrogen-terminated silicon surfaces have attracted a great deal of attention ever since Higashi et al.[3] showed that a simple NH_4F(aq) etching process could produce Si(111) surfaces of unparalleled smoothness and homogeneity on an atomic scale. Interestingly, the perfection of these NH_4F-etched surfaces is profoundly affected by low concentrations (∼ppm) of dissolved O_2 in the etchant, as demonstrated by Wade and Chidsey.[4] Dissolved O_2 also affects the morphologies produced by other silicon etchants, such as NH_3(aq)[5] and KOH(aq).[6] In pure water, dissolved O_2 slowly oxidizes H-terminated silicon surfaces.[7,8] Interestingly, H-terminated surfaces are also readily oxidized by O_2 in humid environments but are surprisingly stable in dry O_2.[7]

In the following, the site-specific reactivity of O_2(aq) toward H-terminated Si(111) is quantified using a combination of experimental measurements of steady-state etch morphologies and atomistic kinetic Monte Carlo simulations of the relevant surface reactions. The reaction products are also identified using polarized infrared absorption spectroscopy of the Si−H stretch vibration.

II. Experimental Section

Two different types of silicon samples were used in these experiments. Since quantitative morphological measurements of site-specific reaction rates require surfaces with a known step density and step orientation,[9] STM experiments were performed on P-doped, 1 Ω cm silicon samples that were miscut from the $(\bar{1}11)$ orientation by 0.35° ± 0.1° toward either the $\langle 11\bar{2}\rangle$ or $\langle \bar{1}\bar{1}2\rangle$ directions. In contrast, surface infrared absorption measurements are best performed in the very surface-sensitive multiple internal reflection geometry.[10] To minimize bulk absorption, infrared absorption measurements were performed on 1000 Ω cm, double-sided-polished silicon samples that were cut to within ±0.5° of the (111) orientation.

Prior to experimentation, the silicon wafers were oxidized in an O_2 atmosphere for 30 min at 1000 °C and then annealed in N_2 for 30 min at 1000 °C. This process produces an ∼1000 Å thick surface oxide layer that engulfs initial surface damage. The 500-μm-thick wafers were then cut with a diamond saw

† Part of the special issue "John C. Tully Festschrift".

* To whom correspondence should be addressed. E-mail: Melissa.Hines@cornell.edu.

10.1021/jp0207073 CCC: $22.00
Published on Web 07/09/2002

TABLE 1: Calculated Concentrations of Species in the Solutions Used in These Experiments

	argon (0% O_2)	air (21% O_2)	oxygen (100% O_2)
$[O_2]$	0	3.0×10^{-4}	1.4×10^{-3}
$[OH^-]$	1.3×10^{-6}	1.3×10^{-6}	1.3×10^{-6}
[HF]	2.5×10^{-4}	2.5×10^{-4}	2.5×10^{-4}

into either 0.6 in. × 0.7 in. samples for STM measurements or 0.6 in. × 1.5 in. samples for infrared absorption measurements. The short faces of the infrared samples were then polished to create 45° bevels. When used in the multiple internal reflection geometry, these samples allow for approximately 76 internal reflections of the infrared radiation.

The morphology and chemical composition of etched silicon samples are extremely sensitive to contamination. To remove gross surface contamination, the samples were degreased in sequential baths of trichloroethylene, acetone, and methanol. Before each experiment, the silicon sample and all labware were scrupulously cleaned using a modified RCA clean.[11] An excellent review of silicon cleaning has been given by Higashi and Chabal.[12] The labware, which was either glass or solid Teflon, was cleaned in a basic peroxide solution (SCA-1) composed of 1:1:4 by volume of 28% NH_3(aq)/30% H_2O_2(aq)/H_2O at 80 °C for at least 10 min, then rinsed thoroughly in running ultrapure water (Millipore Milli-Q). The sample was then cleaned in a fresh SCA-1 bath for 10 min. The thermal oxide was removed from the sample with a 2 min immersion in an aqueous HF/NH_4F solution (Buffer-HF, Transene). After thorough rinsing, the sample was H-terminated, as evidenced by its pronounced hydrophobicity. To ensure cleanliness, a second SCA-1 cleaning was performed. Between each step, the sample was thoroughly rinsed in running ultrapure water.

The morphologies reported in this paper were completely determined by the final processing step—a 30 min etch in a stirred, room temperature 40% NH_4F solution (aq, Transene). During this time, the etch morphology reaches steady state, as confirmed by time-dependent STM observations. The steady-state morphology is highly sensitive to the concentration of O_2 dissolved in the etchant. This concentration was varied by allowing the etchant to equilibrate for 30 min in a flowing atmosphere of research-grade Ar (0% O_2), air (21% O_2), or research-grade O_2 (100% O_2) with vigorous stirring. Table 1 lists the calculated equilibrium concentrations of the reactive species in the solution. After equilibration, the silicon sample was etched in the controlled atmosphere for 30 min with moderate stirring. (Stirring is necessary to ensure etchant homogeneity, which is a prerequisite for our kinetic analysis. The effects of stirring have previously been investigated.[13]) After etching, the sample was removed from the controlled atmosphere and briefly rinsed in ultrapure water. An InGa ohmic contact was applied to the backside of the sample, and the surface was load-locked into an ultrahigh vacuum STM for analysis.

The chemical composition of the etched surfaces was measured using infrared absorption in the multiple internal reflection (MIR) geometry.[10] Infrared radiation from a Fourier transform infrared (FTIR) spectrometer was focused onto the entrance bevel of the sample. The radiation then underwent ~76 surface reflections before exiting the opposite bevel. The transmitted radiation passed through a ZnSe polarizer and then into a MCT detector.

The vibrational spectra of surfaces etched in NH_4F equilibrated with Ar, air, and O_2 environments were indistinguishable. Because of this, a second type of experiment was also performed. In these experiments, the silicon surface was first etched for 6 min in NH_4F. Previous researchers[14] have shown that this etch time is optimal for the production of highly homogeneous H−Si(111) spectra. After rinsing, the etched samples were then immersed for 300 min in stirred ultrapure water in a controlled environment of either pure Ar or pure O_2. This long immersion time allowed any reaction products to build up on the previously etched surface. An infrared spectrum was subsequently obtained. Following this, the etched infrared plates were cleaned in an 80 °C SCA-1 solution to produce an oxidized surface, and a reference spectrum was collected.

III. Results

As previously noted by Wade and Chidsey,[15] dissolved oxygen has a pronounced effect on the morphology of silicon surfaces etched in NH_4F. In the absence of dissolved O_2, NH_4F etching leads to the production of nearly atomically flat Si(111) surfaces. This process has been quantitatively explained in terms of sequential site-specific oxidation and etching reactions.[9] Surfaces that are etched in NH_4F in equilibrium with room air (21% O_2) display a much rougher and more pitted morphology. This dramatic change in etch morphology implies that dissolved O_2 (or a derivative of dissolved O_2, such as O_2^-) must initiate at least one more surface reaction.

In the following, we will first use infrared absorption spectroscopy to show that dissolved oxygen slowly oxidizes the H-terminated surface produced by NH_4F etching. Following this, we will then postulate a site-specific kinetic model to explain the effects of O_2(aq) on NH_4F etching. The kinetic parameters in this model will then be quantified using a combination of experimental STM measurements and kinetic Monte Carlo simulations.

A. Infrared Absorption Measurements. To determine the chemical effects of dissolved O_2, two identically NH_4F-etched silicon samples were immersed in O_2- and Ar-saturated ultrapure water, respectively, for 300 min. The infrared spectra of the water-treated samples were nearly identical over the measured range (~1500−4000 cm^{-1}), except for pronounced differences in the Si−H stretch region (~2050−2300 cm^{-1}). These regions are shown in Figure 1. In the absence of dissolved O_2, immersion in room-temperature water appears to have little chemical effect on the etched surface; the spectrum in Figure 1a is essentially identical to the spectrum of a freshly etched surface (not shown). The most prominent feature in the spectrum is a sharp, p-polarized absorption band at 2083.6 cm^{-1}. Following Jakob and Chabal,[16] we assign this absorption to the Si−H stretch vibration associated with the monohydride terrace. The small, less-polarized absorption features at 2071 and 2135 cm^{-1} are due to a low density of monohydride and dihydride defects, respectively.[16] In this spectrum, the vibrational line width of the Si−H stretch modes is limited by the resolution of the scan (4 cm^{-1}). Importantly, there is no evidence of water-induced back-bond oxidation in O_2-free solutions.

Dissolved oxygen affects the vibrational spectrum in a number of ways, as shown by Figure 1b. First, the dominant Si−H stretch mode is significantly broadened and slightly red-shifted to 2082.3 cm^{-1}. Both of these changes are consistent with the reduced dipole−dipole coupling expected of an inhomogeneous surface.[17,18] The increased intensity in the 2135 cm^{-1} dihydride stretch mode is also indicative of the creation of new defect sites. Second, dissolved O_2 produces a broad absorption feature centered at 2248 cm^{-1} with a full width at half-maximum of 55 cm^{-1}. As pointed out by Lucovsky,[19] electronegative substituents significantly blue shift the Si−H stretch vibration. Using a regression analysis based on the Si−H vibrational frequencies of numerous gas-phase molecules and amorphous

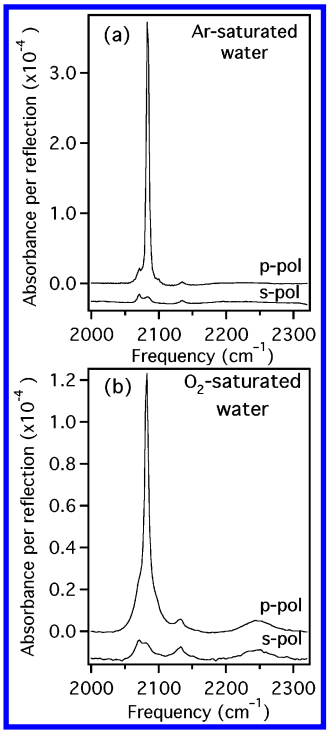

Figure 1. Infrared absorption spectra of H-terminated Si(111) surfaces after 300 min immersion in (a) Ar-saturated and (b) O_2-saturated water. The broad feature centered at 2248 cm^{-1} is assigned to Si−H back-bonded to two or more oxygen atoms, while the features at 2130 cm^{-1} and below are assigned to Si−H back-bonded to silicon (see text).

solids, Lucovsky derived a predictive formula for this inductive shift. These predictions are supported by the observations of Schaefer et al.[20] On the basis of this analysis, we assign this high frequency band primarily to the vibration of monohydride units *triply back-bonded to oxygen*; however, some fraction of this absorption may also be due to the vibration of dihydride units (e.g., step modes) doubly back-bonded to oxygen. Terrace sites with a single oxygen back-bond should have a stretch vibration at ∼2100 cm^{-1}; however, this species cannot be positively identified because of overlap with the dihydride defect mode at 2135 cm^{-1}.

Similar oxidation features have been reported by other researchers. For example, Ogawa et al.[8] also observed the production of a broad feature centered at 2250 cm^{-1} after the prolonged immersion of a H-terminated silicon surface in water containing 8 ppm of dissolved O_2. Similar features have also been reported after extended exposures of H-terminated silicon to dry air or dry O_2.[21−24] These features have also been attributed to O_2-induced back-bond oxidation.

Assuming that the oscillator strength of the Si−H vibration is little affected by inductive shifts, the degree of back-bond oxidation and surface hydrogen coverage can be estimated from the integrated absorption bands. If the s-polarized absorption features are assumed to have an isotropic azimuthal distribution, the total number of Si−H oscillators on a sample, N, is given by

$$N = A(I_p + 2\kappa I_s) \quad (1)$$

where A is a constant related to both the experimental geometry and the Si−H oscillator strength, I_p and I_s are the integrated areas of the absorption band in the p- and s-polarized spectra, and $\kappa = (E_s^2/E_p^2)$, the ratio of the squared surface electric fields in the s- and p-polarized geometries. For the case of a Si−H oscillator measured in our MIR geometry, Chabal has estimated that $\kappa \approx 1.55$.[25]

The degree of back-bond oxidation can be roughly estimated from a comparison of the integrated absorption intensity between 2145 and 2300 cm^{-1}, which is due to multiply oxidized species, to that of the entire Si−H absorption band (2040−2300 cm^{-1}). From this, we estimate that 25% of the Si−H oscillators are multiply back-bonded to oxygen after a 300 min exposure to O_2-saturated water (Figure 1b). In contrast, no oxidation is observed after a similar exposure to Ar-saturated water, as shown by Figure 1a.

Interestingly, there is *no evidence* of H-loss after exposure to O_2-saturated water. In fact, a numerical analysis suggests that the density of H actually increases! We are, however, cautious in our interpretation of this increase, because the magnitude of the increase depends sensitively on both the assumed isotropy of the *s*-polarized absorption band and the magnitude of κ. On the other hand, increased surface H would be consistent with a somewhat roughened surface. An increase in the integrated Si−H absorption in unpolarized spectra has also been reported by Ogawa et al.,[8] who studied much longer exposures ($\leq 10^5$ min) of H-terminated Si(111) to dissolved O_2. During these ultralong exposures, though, the etching of silicon by water cannot be neglected, and water etching reactions likely remove many monolayers of silicon.[7]

Dissolved O_2 does not lead to the production of silanol species. Samples immersed in Ar- and O_2-saturated water develop small absorption features in the 3600−3775 cm^{-1} range; however, samples from O_2-saturated solutions do not consistently show more silanol than those from Ar-saturated solutions.

In summary, dissolved O_2 leads to the insertion of O atoms into Si−Si back-bonds, with little to no loss of the H-termination. No other stable products are observed. Unfortunately, our use of the MIR geometry precludes our quantification of the extent of oxidation, as strong multiphonon absorption features obscure the crucial Si−O stretch region near 1100 cm^{-1}.

B. Morphological Studies. The steady-state morphology of an etched surface is a direct reflection of the reactivity of the chemical etchant. Because of this, the site-specific rates of chemical etching can be quantified from a study of the etch morphology.

In O_2-free solutions, NH_4F etching leads to the production of nearly atomically flat surfaces as shown by the STM images in Figure 2a1,c1. Si(111) surfaces have two principal miscuts and thus two principal step structures. As illustrated by Figure 3, surfaces miscut toward the $\langle 11\bar{2}\rangle$ direction etch to form steps with a monohydride termination, while surfaces miscut toward the $\langle \bar{1}\bar{1}2\rangle$ direction etch to form dihydride-terminated steps. (The step structures were originally determined from detailed spectroscopic studies.[16,26,27])

The production of nearly atomically flat Si(111) surfaces by (O_2-free) NH_4F etching has been previously explained[9] in terms of sequential oxidation and etching of individual silicon atoms:

$$\equiv\text{Si}-\text{H(ads)} + \text{OH}^-\text{(aq)} + \text{H}_2\text{O} \rightarrow \equiv\text{Si}-\text{OH(ads)} + \text{H}_2\text{(g)} + \text{OH}^-\text{(aq)} \quad (2)$$

$$(\equiv\text{Si})_3\text{Si-OH(ads)} + 3\text{HF(aq)} \rightarrow 3(\equiv\text{Si}-\text{H})\text{(ads)} + \text{SiF}_3\text{OH(aq)} \quad (3)$$

As in most aqueous silicon etchants, oxidation, rxn 2, is the rate-limiting reaction. In this etchant, oxidation is highly site-specific; the most reactive silicon site, a kink site, is over 7

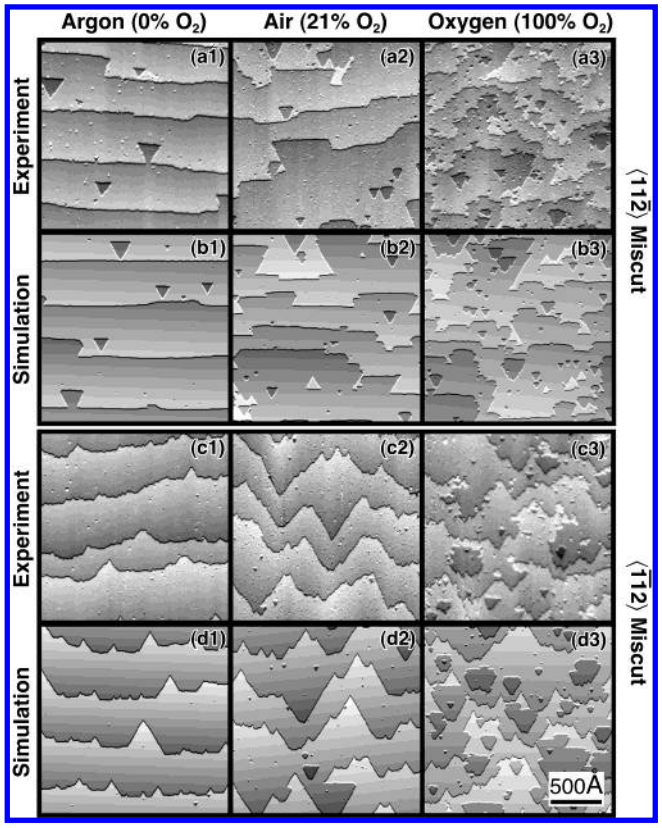

Figure 2. Observed (a, c) and simulated (b, d) steady-state etch morphologies of Si(111) surfaces etched in NH_4F solutions with varying amounts of dissolved O_2. The surface is miscut toward the $\langle 11\bar{2}\rangle$ direction in rows a and b and toward the $\langle \bar{1}12\rangle$ direction in rows c and d. During etching, the stirred NH_4F solutions were in equilibrium with atmospheres of Ar (column 1), air (column 2), and O_2 (column 3).

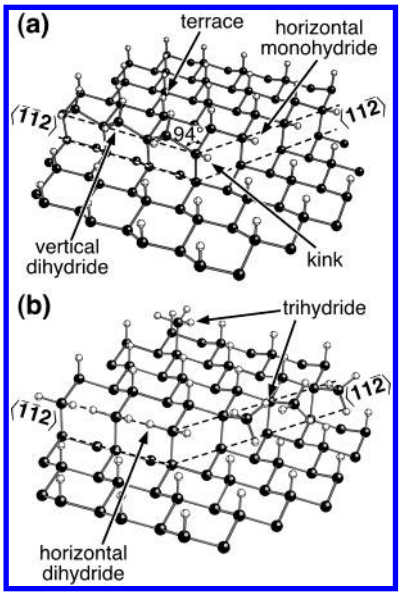

Figure 3. The atomic structure of Si(111) surfaces etched in aqueous solutions. The dark balls represent Si atoms, while the light balls represent H atoms: (a) sites that have been identified by vibrational spectroscopy; (b) transient species.

orders of magnitude more reactive than the least reactive site, the terrace site. This pronounced anisotropy was previously explained in terms of the presumed transition state to rxn 2.

When O_2 is dissolved in the etchant, a dramatic change in the steady-state etch morphology is observed, as shown by the STM images in Figure 2. Since dissolved O_2 presumably has

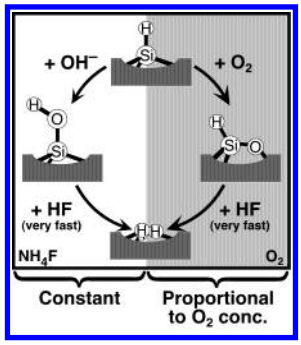

Figure 4. In solutions containing both dissolved O_2 and NH_4F, two reaction channels are open to the etching surface. The relative importance of the two channels is controlled by the O_2 concentration.

no effect on the NH_4F solution itself, we attribute these morphological changes to additional O_2-induced site-specific reactions. The spectroscopic data in section A suggest that O_2 first oxidizes individual silicon sites, then HF in the NH_4F solution etches the oxidized site. O_2-induced oxidation is presumably rate-limiting, as no oxidized species are observed in the infrared spectra of surfaces etched in O_2-saturated NH_4F.

The etching of Si(111) surfaces in NH_4F solutions containing dissolved O_2 can thus be viewed as a kinetic competition between two site-specific reaction pathways, as sketched in Figure 4. The relative importance of the two pathways can be controlled by varying the partial pressure of O_2 above the solution and thus the (equilibrium) concentration of dissolved O_2.

In the following, we will quantify the site-specific rates of O_2-induced oxidation of Si(111) by characterizing the O_2-concentration-dependent changes in the etch morphology using a combination of STM imaging and kinetic Monte Carlo simulations.

1. STM Studies. The major trends in O_2 reactivity can be inferred from a visual inspection of the experimental morphologies in Figure 2. In the absence of O_2, NH_4F etching leads to the production of atomically flat terraces separated by relatively straight vicinal steps. Straight steps are the hallmark of rapid kink etching.[28] Kinks are nucleated when a single atom is removed from a straight step segment. If kink etching is much faster than kink nucleation, the nucleated kink will etch rapidly, creating a new kink at the neighboring site. Rapid sequential kink etching leads to rapid "unzipping" of the step edge and the production of relatively straight steps. In contrast, if the rate of kink nucleation (i.e., step etching) is comparable to the rate of kink etching, a ragged step morphology will result. The relatively straight steps in Figure 2a1,c1 immediately suggest that kink etching in pure NH_4F(aq) is orders of magnitude faster than the etching of either the monohydride- or dihydride-terminated steps.[28]

The triangular etch pits in Figure 2a1 give a second clue to the highly anisotropic nature of (O_2-free) NH_4F etching. Etch pits are bounded by atomic step segments, so the pit shape is determined by the relative rates of step etching. Si(111) is a 3-fold symmetric surface with two different types of steps: monohydride-terminated and dihydride-terminated. If the two step types have equal etch rates, the etch pits will be either hexagonal (fast kink etching) or amorphous (slow kink etching). When one type of step etches faster than the other, triangular pits, which are bounded by the slow etching step, result. The orientation and pronounced triangularity of the pits in Figure 2a1 suggest that the dihydride-terminated steps etch at least 1

order of magnitude more quickly than the monohydride-terminated steps in pure NH_4F.[28]

The relatively low density of etch pits on NH_4F-etched surfaces is indicative of a relatively small terrace etch rate. Because etching steps engulf etch pits in their path, the etch pit density is determined by a competition between etch pit nucleation, which is controlled by the terrace etch rate, and etch pit annihilation, which is controlled by the step etch rate. In the case of NH_4F etching, surfaces miscut to produce the slow etching, monohydride-terminated steps (Figure 2a1) have a higher density of etch pits than surfaces miscut to produce fast etching, dihydride-terminated steps (Figure 2c1). These two images also illustrate the subtle information that can be conveyed by etch morphologies. The surfaces in Figure 2a1,c1 were produced with *identical* rates of terrace etching, and the differences in pit density are solely due to the different step etch rates.

When dissolved O_2 is introduced by changing the composition of the atmosphere above the etchant, all of the characteristic etch features change significantly. As seen in the experimental morphologies in Figure 2a2,a3,c2,c3, the steps become more ragged, while the etch pits increase in number and become less triangular. The increased pit density implies that dissolved O_2 attacks the relatively unreactive terrace sites, while the change in pit shape suggests that dissolved O_2 must also attack the step sites. The increased roughness of the etched surface also indicates that dissolved O_2 is somewhat less anisotropic (i.e., site-specific) than NH_4F.

Although a visual inspection yields *qualitative* information about the reactivity of dissolved O_2, *quantitative* information is difficult to infer. As the surface etches, the various morphological features (e.g., steps, pits) interact with one another. Because of this, individual features cannot be analyzed in isolation. For example, the change in etch pit density cannot be directly related to a change in terrace etch rate, since the etch pit density is also influenced by the step etch rate. Because of this, quantitative conclusions require rigorous simulation, which is the subject of the next section.

2. Kinetic Monte Carlo Simulations. To quantify the experimental morphologies, the etch chemistry was modeled with an atomistic, kinetic Monte Carlo simulation of Si(111) etching, which has been previously described.[28] This model incorporates the full structure of the Si(111) lattice, including the interlayer stacking pattern, and all possible reactive sites within the solid-on-solid approximation. The surface sites were classified according to their structure into seven chemically distinct species: terrace, vertical dihydride step, horizontal monohydride step, kink, trihydride, horizontal dihydride, and point.[29]

In the O_2-containing NH_4F solutions modeled by the simulations, individual silicon sites are etched by sequential oxidation and etching reactions, which can be initiated either by the etchant (NH_4F) or by the dissolved O_2. These competing reaction channels are illustrated by Figure 4. In the first step, a H-terminated silicon site is either oxidized by OH^- to produce a surface silanol species (rxn 2) or by dissolved O_2 to produce a H-terminated silicon site back-bonded to oxygen. In both of these cases, the Si−Si back-bonds of the oxidized silicon atom are weakened by the strongly electron-withdrawing oxygen atom and HF etching rapidly removes the oxidized site and regenerates the H-termination.[30]

Although 28 site-specific reaction rates are needed to completely describe these four reaction channels, a number of simplifying assumptions can be made. Since the infrared absorption experiments strongly suggest that oxidation is rate-limiting in these experiments, we assumed that the etching reactions were infinitely fast. Because of this, the steady-state morphology is controlled by the 14 site-specific oxidation rates. In addition, trihydride and horizontal dihydride species have never been observed in the infrared spectra of NH_4F-etched samples. Because of this, we assumed that the oxidation of both the trihydride and horizontal dihydride sites was infinitely fast compared to the oxidation of other sites. Taking these approximations into account, only 10 site-specific oxidation rates were needed. Since our experiments were performed in a well-stirred solution, we further assumed that the solution-phase reactants were isotropically distributed and in equilibrium with the controlled atmosphere. For a given O_2 partial pressure, P_{O_2}, the 10 site-specific rates of oxidation can be reduced to five effective site-specific rates of etching, k^i, which are given by

$$k^i = k^i_{OH} + k^i_{Ox}\frac{P_{O_2}}{P^0} \tag{4}$$

where k^i_{OH} is the rate of oxidation of site i by OH^-, k^i_{Ox} is the rate of oxidation of site i by dissolved O_2 in a O_2-saturated solution, and P^0 is atmospheric pressure.

During the simulation, single atoms were randomly etched (i.e., removed) from the surface subject to the site-specific etch rates, k^i. Toroidal bounds were used to simulate an infinite surface. Diffusion of surface atoms and redeposition of etch products were not allowed. Both of these approximations are excellent in room-temperature aqueous solutions. The simulation was allowed to etch to steady state, and then the experimental and simulated morphologies were visually compared. Using an iterative approach, we adjusted the 10 site-specific rates of oxidation until a satisfactory fit with experiment was obtained. In judging the quality of the fit, particular attention was paid to the size, shape, and density of the etch pits, as well as to the step edge morphology. During the fitting process, at least six representative experimental and simulated images were studied for each set of reaction conditions.

TABLE 2: Measured Site-Specific Rates of Oxidation of H-Terminated Si(111) Sites by OH^- and Dissolved O_2[a]

site	rate of OH^- attack (k_{OH})	rate of O_2 attack (k_{Ox})
kink	1	≤ 0.1
point	0.1	≤ 0.01
dihydride step	0.01	0.04
monohydride step	0.0005	0.01
terrace	4×10^{-8}	1.5×10^{-6}

[a] The reaction mechanism is illustrated in Figure 3.

The best-fit simulated morphologies are displayed in Figure 2b,d. All six of the simulated morphologies were generated with the *same set* of site-specific reaction rates; only the surface miscut and P_{O_2}, which are known from experiment, were varied. The best-fit site-specific rate constants for oxidation by OH^- (i.e., rxn 2) and by O_2(aq) are listed in Table 2. At the relatively low O_2 concentrations studied here, dissolved O_2 does not significantly change the overall rates of kink and point site oxidation. Because of this, only upper bounds for these rates can be determined.

The simulated morphologies are very sensitive to changes in the site-specific rates. In general, varying any one rate by a factor of 3 generates only a minor change in the final morphologies, but larger changes or changes in more than one rate lead to degradation of the fit. To illustrate this sensitivity, Figure 5 shows two experimental and six simulated morphologies. The simulated morphologies differ only in the rate of terrace site

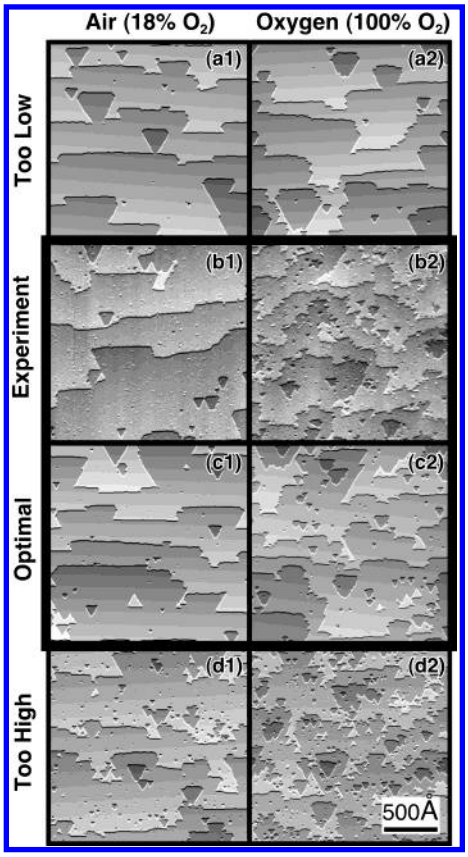

Figure 5. Illustration of the sensitivity of the simulated morphologies to changes in the site-specific etch rates. Row b shows the experimental morphologies obtained from two experiments on $\langle 11\bar{2}\rangle$-miscut surfaces, while row c represents the best fit simulation using the parameters in Table 2. The simulated morphologies in rows a and d were generated using the same parameters as those in row c except for one rate: row a used a terrace etch rate 10 times too low (i.e., 1.5×10^{-7}), while row d used a terrace etch rate 10 times too high (i.e., 1.5×10^{-5}).

oxidation by O_2; all other rate constants were held constant. The simulations in row a were generated by a rate constant 10 times lower than the optimal constant. The simulations in row c were generated by the optimal rate constant, and the simulations in row d were generated by a rate constant 10 times larger than the optimal constant. In evaluating the simulated morphologies, it is important to remember that the optimal parameters must reproduce both the specific morphology *and* the observed concentration dependence. In other words, the quality of fit to both experimental images (Figure 5b1,b2) must be judged *simultaneously*.

Figure 5 shows that the optimal rate constant is readily distinguished from the nonoptimal parameters. When the terrace oxidation rate is too low, the simulated etch pits are much too large and also too few in number as shown by Figure 5a1,a2. In contrast, when the terrace oxidation rate is too high, there are far too many tiny etch pits, as seen in Figure 5d1. These images also illustrate the importance of studying more than one concentration. For example, the etch pit density in Figure 5b2 is arguably intermediate between Figure 5 parts c2 and d2; however, Figure 5b1 is clearly in better agreement with Figure 5c1 than with Figure 5d1.

As expected from the etch morphologies, the measured rate constants show that dissolved O_2 is a less anisotropic reactant than OH^-. In pure NH_4F, the site-specific rates of oxidation span more than 7 orders of magnitude. In contrast, the site-specific rates of oxidation by dissolved O_2 span at most 5 orders of magnitude. Nevertheless, the patterns of reactivity are quite similar. Both species attack defect sites, such as kinks and steps, much more rapidly than they attack the majority species, the terrace site. In terms of absolute reactivity, OH^- is much more reactive than O_2. In O_2-saturated solutions, the concentration of dissolved oxygen is approximately 1000 times higher than the concentration of OH^- as shown by Table 1.

IV. Discussion

Taken together, the morphological and spectroscopic data are consistent with a mechanism in which dissolved O_2 first oxidizes a surface back-bond to form a Si−O−Si moiety. This reaction is site-specific; reaction at kink and step sites is preferred over reaction at terraces. This reaction is not, however, as anisotropic as oxidation in pure NH_4F. After oxidation, the oxidized silicon atom is rapidly removed by HF etching. This reaction regenerates the H-terminated surface. The proposed reaction scheme is illustrated by Figure 4.

What determines the site-specificity of the O_2-induced oxidation pathway? Some insight can be gained from the organosilicon literature. Linear organopolysilanes are stable to atmospheric oxidation, but cyclic analogues react rapidly with O_2 (in organic solvents) to form siloxanes.[31,32] In almost every case, oxidation by O_2 inserts a single oxygen atom into a Si−Si bond.[32] This insertion reaction is facile regardless of the functional groups bound to the silicon atoms; the important criterion is that the Si−Si bond be part of a ring. Because of this, O_2-induced oxidation is thought to be activated by ring strain.

This reactivity pattern is similar to the one presented in Table 2. The structure of H-terminated Si(111) surfaces has been previously studied in great detail, both experimentally[16,26,33] and theoretically.[27] On the basis of these studies, the relative strain in the surface sites is expected to be kink > dihydride step > monohydride step ≈ point > terrace. At least qualitatively, the O_2 reactivity in Table 2 also follows this pattern. Because of this, we tentatively ascribe the observed trends in O_2 site-specific reactivity to strain.

This reactivity pattern is significantly different from that observed in pure NH_4F etching, in which the reactivity is poorly correlated with site strain. For example, in NH_4F, the unstrained point site is approximately 1 order of magnitude more reactive than the highly strained dihydride step site. Oxidation by OH^-, which is thought to be the rate-limiting reaction in NH_4F etching, is believed to proceed through a bimolecular, front-side attack mechanism.[33] Hines has previously argued that the observed reactivity of NH_4F etching can be explained in terms of the ease of accessing the presumed pentavalent transition state for this reaction.[9]

Water apparently plays a crucial role in O_2-induced oxidation of H-terminated silicon surfaces, as pointed out by Morita et al.[7] and confirmed by others.[21,22] Zhang et al. have performed detailed kinetic studies of the reaction of pure O_2(g) with H-terminated Si(100)[34] and Si(111)[35] surfaces at 300 °C. Like the system studied here, Zhang et al. found that O_2 leads to oxidation of Si−Si back-bonds with no loss of H-termination and no production of silanol species. Zhang et al. also found that the relative rates of O_2(g)-induced oxidation are dihydride step > monohydride step > terrace, which also agrees well with our observations. (Meaningful comparisons of the magnitude of the anisotropy cannot be made, because Zhang's experiments were performed at elevated temperature.) In stark contrast to our results, the oxidation of H-terminated silicon by O_2(g) proceeds at a negligible rate at room temperature. In fact, the data of Zhang et al. suggest that only 10% of a H-terminated silicon surface would be oxidized after a half-millennium

exposure to room-temperature air! Presumably, the huge difference in oxidation rates between dissolved O_2 and O_2 gas is due to the stabilizing or solvating effect of water. Indeed, previous researchers have found that H-terminated surfaces oxidize much more quickly in humid environments than in dry environments.[7,21,22]

Although the site-specific rates of H−Si(111) oxidation by O_2(g) and by dissolved O_2 show similar trends, this observation does not necessarily imply that the reactions proceed by similar mechanisms. In fact, Morita et al.[7] have noticed pronounced differences in the *multilayer* oxidation kinetics of these two species, suggesting that oxidation by O_2(g) and by O_2(aq) proceed through different mechanisms when a significant oxide layer is present.

Wade and Chidsey[4] have suggested that the reactivity of dissolved O_2 is actually due to the production of superoxide anion radicals (O_2^-) by the etching surface. During etching, the silicon surface develops a "corrosion potential" sufficient to reduce O_2 to O_2^-. If this species is indeed formed at the silicon surface, Wade and Chidsey argue that the superoxide ions could abstract hydrogen from the H-terminated surface, thereby creating a silicon radical. The highly reactive radical would then undergo further reaction, presumably with water. This mechanism also explains the low reactivity of dry O_2(g) toward H-terminated silicon, as liquid water is needed to solvate the proposed radical anion.

Our kinetic model cannot directly distinguish reactions initiated by O_2 from those initiated by an O_2-derived species, such as the superoxide ion. Nevertheless, the observed reactivity is somewhat different from what we would expect of the proposed radical-initiated reaction. First, the infrared spectra strongly suggest that oxidation of the surface back-bonds dominates, and there is no evidence of hydrogen loss after prolonged exposure to dissolved oxygen. These observations are difficult to reconcile with a H-abstraction mechanism. Second, dissolved O_2 leads to anisotropic oxidation; step sites are approximately 10^4 times more reactive than terrace sites. Presumably, this anisotropy is indicative of a significant activation barrier to reaction, which is counterintuitive for a radical-initiated mechanism. We note, however, that the proposed electrochemical production of O_2^- could itself be anisotropic. For example, the production of O_2^- might be faster at step sites than at terrace sites.

V. Conclusions

The site-specific oxidation rates of a very dilute impurity species, dissolved O_2, can be quantified from changes in the steady-state etch morphology as a function of impurity concentration. In the absence of the impurity, the steady-state etch morphology reflects the site-specific reactivity of the pure etchant. As the concentration of the impurity is increased, changes in the steady-state etch morphology are observed. By comparing concentration-dependent kinetic Monte Carlo simulations of the site-specific oxidation and etching reactions to the observed steady-state etch morphologies, site-specific rates of chemical reaction can be extracted.

Dissolved O_2 is a rather anisotropic oxidant of H-terminated Si(111). For example, step sites are oxidized 10^4 times more rapidly than terrace sites. This anisotropy is tentatively attributed to site-specific differences in bond strain, as strained sites are more susceptible to oxidation than unstrained sites. Similar trends in O_2-induced oxidation have been observed in organopolysilanes. Spectroscopic studies of etched, H-terminated silicon surfaces show that dissolved O_2 leads to the insertion of O atoms into surface back-bonds without significant loss of H-termination. Surface silanols are not formed by this reaction. Similar trends have been observed in the reactivity of O_2(g) with both Si(111) and polysilanes.

Acknowledgment. This material was supported in part by the NSF under Award No. CHE-9733165. Acknowledgment is also made to the donors of the Petroleum Research Fund, administered by the American Chemical Society, for partial support of this research. This work made use of the Cornell Center for Materials Research Shared Experimental Facilities, supported through the National Science Foundation Materials Research Science and Engineering Centers program (Grant DMR-9632275).

References and Notes

(1) Sangwal, K. *J. Cryst. Growth* **1993**, *128*, 1236.
(2) Sangwal, K. *Etching of Crystals*; North-Holland: Amsterdam, 1987; Chapter 7.
(3) Higashi, G. S.; Chabal, Y. J.; Trucks, G. W.; Raghavachari, K. *Appl. Phys. Lett.* **1990**, *56*, 656.
(4) Wade, C. P.; Chidsey, C. E. D. *Appl. Phys. Lett.* **1997**, *71*, 1679.
(5) Fukidome, H.; Matsumura, M. *Surf. Sci.* **2000**, *463*, L649.
(6) Campbell, S. A.; Cooper, K.; Dixon, L.; Earwaker, R.; Port, S. N.; Schiffrin, D. J. *J. Micromech. Microeng.* **1995**, *5*, 209.
(7) Morita, M.; Ohmi, T.; Hasegawa, E.; Kawakami, M.; Ohwada, M. *J. Appl. Phys.* **1990**, *68*, 1272.
(8) Ogawa, H.; Ishikawa, K.; Inomata, C.; Fujimura, S. *J. Appl. Phys.* **1996**, *79*, 472.
(9) Hines, M. A. *Int. Rev. Phys. Chem.* **2001**, *20*, 645.
(10) Chabal, Y. J. *Surf. Sci. Rep.* **1988**, *8*, 211.
(11) Kern, W.; Puotinen, D. *RCA Rev.* **1970**, *31*, 187.
(12) Higashi, G. S.; Chabal, Y. J. In *Handbook of Semiconductor Wafer Cleaning Technology*; Kern, W., Ed.; Noyes: Park Ridge, NJ, 1993; p 433.
(13) Huang, Y.-C.; Flidr, J.; Newton, T. A.; Hines, M. A. *Phys. Rev. Lett.* **1998**, *80*, 4462.
(14) Jakob, P.; Dumas, P.; Chabal, Y. J. *Appl. Phys. Lett.* **1991**, *59*, 2968.
(15) Wade, C. P.; Chidsey, C. E. D. *Mater. Res. Symp. Proc.* **1997**, *477*, 299.
(16) Jakob, P.; Chabal, Y. J. *J. Chem. Phys.* **1991**, *95*, 2897.
(17) Jakob, P.; Chabal, Y. J.; Raghavachari, K. *Chem. Phys. Lett.* **1991**, *187*, 325.
(18) Newton, T. A.; Boiani, J. A.; Hines, M. A. *Surf. Sci.* **1999**, *430*, 67.
(19) Lucovsky, G. *Solid State Commun.* **1979**, *29*, 571.
(20) Schaefer, J. A.; Frankel, D.; Stucki, F.; Göpel, W.; Lapeyre, G. J. *Surf. Sci.* **1984**, *139*, L209.
(21) Niwano, M.; Kageyama, J.; Kurita, K.; Kinashi, K.; Takahashi, I.; Miyamoto, N. *J. Appl. Phys.* **1994**, *76*, 2157.
(22) Miura, T.; Niwano, M.; Shoji, D.; Miyamoto, N. *J. Appl. Phys.* **1996**, *79*, 4373.
(23) Hattori, T.; Aiba, T.; Iijima, E.; Okube, Y.; Nohira, H.; Katayama, M.; Tate, N. *Appl. Surf. Sci.* **1996**, *104*/*105*, 323.
(24) Hattori, T.; Nohira, H. In *Fundamental Aspects of Silicon Oxidation*; Chabal, Y. J., Ed.; Springer: Berlin, 2001; p 61.
(25) Chabal, Y. J. In *Semiconductor Interfaces: Formation and Properties*; LeLay, G., Derrien, J., Eds.; Springer-Verlag: Berlin, 1987; Vol. 22, p 301.
(26) Jakob, P.; Chabal, Y. J.; Kuhnke, K.; Christman, S. B. *Surf. Sci.* **1994**, *302*, 49.
(27) Raghavachari, K.; Jakob, P.; Chabal, Y. J. *Chem. Phys. Lett.* **1993**, *206*, 156.
(28) Flidr, J.; Huang, Y.-C.; Newton, T. A.; Hines, M. A. *J. Chem. Phys.* **1998**, *108*, 5542.
(29) Flidr, J.; Huang, Y.-C.; Hines, M. A. *J. Chem. Phys.* **1999**, *111*, *6970*.
(30) Trucks, G. W.; Raghavachari, K.; Higashi, G. S.; Chabal, Y. J. *Phys. Rev. Lett.* **1990**, *65*, 504.
(31) Kumada, M.; Tamao, K. *Adv. Organomet. Chem.* **1968**, *6*, 19.
(32) West, R. In *The Chemistry of Organic Silicon Compounds*; Patai, S., Rappaport, Z., Eds; Wiley: New York, 1989; Chapter 19.
(33) Hines, M. A.; Chabal, Y. J.; Harris, T. D.; Harris, A. L. *J. Chem. Phys.* **1994**, *101*, 8055.
(34) Zhang, X.; Garfunkel, E.; Chabal, Y. J.; Christman, S. B.; Chaban, E. E. *Appl. Phys. Lett.* **2001**, *79*, 4051.
(35) Zhang, X.; Chabal, Y. J.; Christman, S. B.; Chaban, E. E.; Garfunkel, E. *J. Vac. Sci. Technol.* **2001**, *A19*, 1725.